

Proceedings of the 9th International Conference on Cyclotrons and their Applications
September 1981, Caen, France

IPN ORSAY PROJECT - FIRST MACHINE DESIGN STUDIES

A. Laisné

Institut de Physique Nucléaire, B.P. n° 1, 91406 Orsay cedex, France

Abstract.- After a brief presentation of the proposal of the "Institut de Physique Nucléaire d'Orsay this paper describes the main guidelines which have been chosen in the first design studies of an ISOCRONOUS CYCLOTRON WITH SUPERCONDUCTING COILS.

1. General description of the "IPN ORSAY" proposal.- In our laboratory experimental studies in the field of Nuclear Physics and connected areas are developed around three accelerator facilities.

The ALICE system which consists of a LINAC coupled with a variable energy cyclotron (K = 70). This accelerator system provides heavy ion beams (¹²C to ⁸⁴Kr) with maximum energies of 18 MeV/A (C) to 6 MeV/A (Kr).

The MP Tandem is a "HVEC" electrostatic machine with a maximum terminal voltage of 13. MV. Both, light ions (p,d,He) up to 30 - 40 MeV and Heavy ions (C. to Ni) beams are accelerated by this machine.

The new Synchrocyclotron SC 200 (K ≈ 220), which has been recently rebuilt by the laboratory staff, produces protons with variable energy between 166 and 200 MeV and other light particles with Z/A = 0.5 at a maximum energy of 50 MeV per Nucleon.

Taking into account the characteristics of these machines and the different subfields of nuclear Physics developed at ORSAY the goal of our laboratory for the years 1988-1990 is to replace the existing machines by a modern unique and flexible accelerator system which will have the following capabilities.

The central part of the proposal is a compact isochronous cyclotron with superconducting coils used as a "clean accelerator" associated with 3 external ion sources. The main parameters of the cyclotron are listed below (Table II), while table III, summarizes the characteristics of the external beams providers.

TABLE 2

Max Bending constant $K_B = 600$	$T_{MAX} \left(\frac{Z_i}{A}\right) = K_B \cdot x \left(\frac{Z_i}{A}\right)^2$ for $\frac{Z_i}{A} \leq \frac{K_F}{K_B} = 0.37$
Min " " $K_{Bm} = 111$	$T_{MAX} \left(\frac{Z_i}{A}\right) = K_F \times \frac{Z_i}{A}$ for $\frac{Z_i}{A} > 0.37$
Focusing constant $K_F = 222$	
Sector number	3
Average magnetic field	4.05 - 1.75 Tesla
Extraction Radius	0,87 m
RF Frequency Range	24-62 MHz
Harmonic operating modes	2, 3, 4
Electrode Peak Voltage	100. KV
Internal ion source	NO
Pole Radius	0.94 m
Hill Gap (constant)	0,07 m
Valley profile	modified ellipsoid
Yoke height	≈ 3.8 m
Inner and outer Yoke radii	1.4 - 2
Total Weight	≈ 300. Ton

TABLE 1

Light ions	$T \approx 40-200$ MeV protons(p and \bar{p})	$\left\{ \begin{array}{l} \frac{\Delta T}{T} = 5 \cdot 10^{-4} \\ \epsilon \leq \pi \cdot \text{mm} \times \text{mrad} \\ i \approx 10^{12} - 10^{13} \text{ pps} \end{array} \right.$	} Macro duty cycle ≈ 100%
	with \bar{d}	$\left\{ \begin{array}{l} \frac{\Delta T}{T} = 5 \cdot 10^{-4} \\ \epsilon \leq \pi \cdot \text{mm} \cdot \text{mrad} \\ i \approx 1.10^{10} \text{ up to } 5 \times 10^{11} \text{ pps} \end{array} \right.$	
	$T \approx 4 - 100$ MeV/A up to $A=40$	$\left\{ \begin{array}{l} \frac{\Delta T}{T} \approx 10^{-3} \\ i \approx 10^9 \text{ up to } 5 \times 10^{10} \text{ pps} \end{array} \right.$	
Heavy ions	$T \approx 4-80$ MeV/A up to $A \approx 80$	$\left\{ \begin{array}{l} \frac{\Delta T}{T} \approx 10^{-3} \\ i \approx 10^9 \text{ up to } 5 \times 10^{10} \text{ pps} \end{array} \right.$	
	$T \approx 4-50$ MeV/A up to $A \approx 200$	Macro duty cycle ≈ 30%	

TABLE 3 : External ion sources

Radial Injection : MP Tandem, upgraded to 15 MV. Heavy ions from (C) to (U) with a macro duty cycle of 100 % providing at the exit of the machine intensities in the range 3.7 to 1.2×10^{11} pps

Axial Injection : from a Plat-form at 36 kV Max equipped with

- 1) a classical DUOPLASMATRON for light Ions only
- 2) an Electron beam ion source (CRYEBIS III)

The operating diagram of the cyclotron in MeV/n, $T_{\min} - T_{\max}$ versus the charge to mass ratio Z_i/A of the accelerated ions is shown Fig(1).

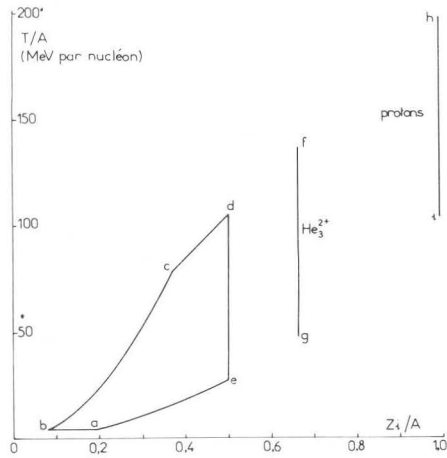


Fig. 1 : Kinetic energy T (MeV/n) versus charge to mass ratio Z_i/A of the IPN ORSAY proposal.

2. Average magnetic field range.- A previous study used a conventional average field ranging between 2.06 T and 4.7 T, associated with an extraction radius of 0.75 m.

The maximum RF frequency needed for proton acceleration up to 200 MeV was 72 MHz ($h = 2$) in order to reach a natural turn separation of 1.3 mm at $v_x = 0.9$.

The study of Axial injection using an electrostatic mirror as an inflector revealed the importance of the parameter

$$P = \frac{Z_i}{A} \cdot B(0)^2$$

which is related to the square of the radius of curvature ρ of an injected ion of kinetic energy V by

$$\rho^2 = \frac{V}{P}$$

The maximum central field $B(0)_{\max}$ then leads to a maximum value P of 7, and to the impossibility of discovering outgoing trajectories from the centered mirror with radii of curvature greater than 8 mm. This turns out to be inadequate with the 10 mm electric gaps and the necessity to link up with accelerated equilibrium orbits.

We therefore, find it necessary to lower the average magnetic field range to

$$1.75 \text{ Tesla} < \tilde{B}_{\text{extr}} < 4.03 \text{ Tesla}$$

which is associated with an extraction radius

$$r_{\text{ext}} = 0.87 \text{ m.}$$

The present choice leads to $P_{\max} = 5.16$ which is low enough for allowing reasonable curvature radii (11.5 - 16.5 mm) and angles of trajectories with the normal to the electric gaps less than 42° (1).

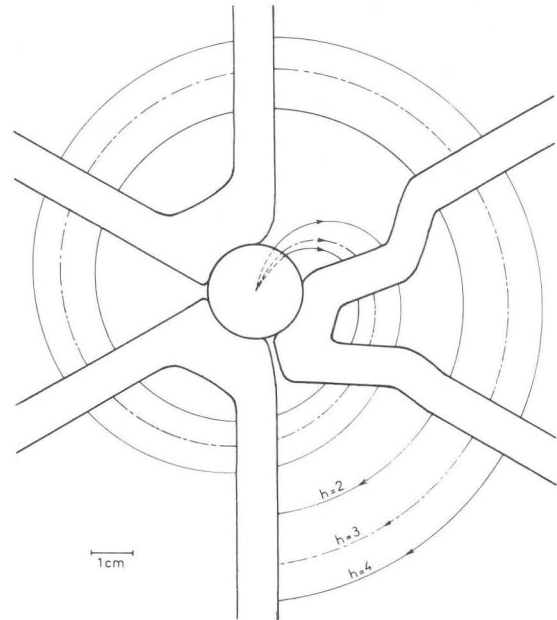


Fig. 2 : Constant trajectories in the median plane corresponding to each accelerating harmonic mode, and shapes of the first accelerating gaps. The injected beams are supposed to travel on the vertical axis of the machine.

A schematic representation of this central geometry is shown in Fig. (2). The variation of the parameter P versus the charge to mass ratio Z_i/A for different harmonic modes is represented in Fig. (3).

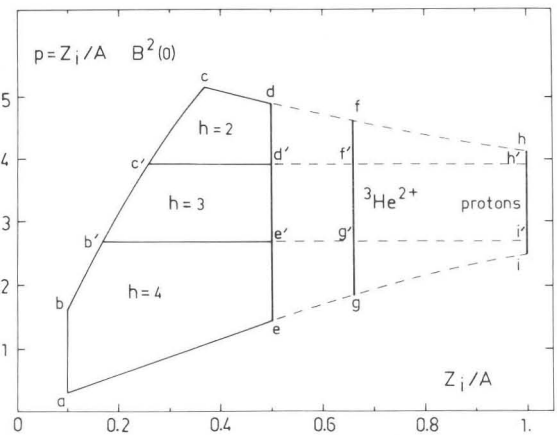


Fig. 3 : "P" parameter versus " Z_i/A " for the different harmonic modes.

Under such conditions the maximum vertical electric field component in the mirror is limited to about 30.KV/cm, see Fig. (4).

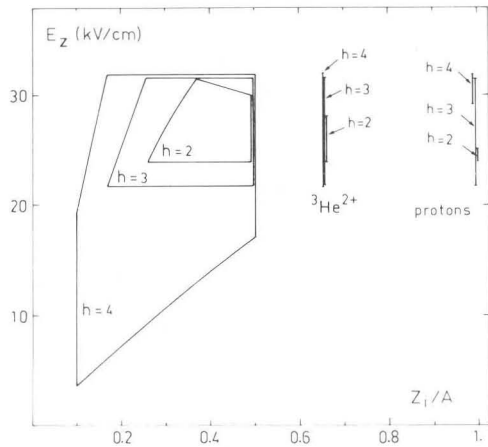


Fig. 4 : Vertical electric component in the mirror as an inflector versus Z_1/A for the different harmonic modes.

Two other obvious consequences of this last choice are : the maximum RF frequency is lowered to 62 MHz and the radial turn separation at the extraction radius increased to 1.54 mm.

3. General Guidelines.— Considering the lack of accurate information on the general guidelines which have been followed by the first designers as regard to the shape of the iron profile, the shape, position and partition of the main coils, the height and diameter of the yoke, I will attempt to present here in some detail the guidelines which have been selected in the present.

3.1.— First order assumptions and main coil partition.— At first, disregarding the flutter effect, we considered the mean fields to be realized as equal to

$$\tilde{B}(r) = B(o).\gamma(r).$$

We observed the amazing similarity of this radial behavior with that created by coils close to the median plane.

- Using the fact we can choose electrical densities as high as 3 500 A/cm² and making use of code which calculates the position of a circular coil to fit a given magnetic field law $\tilde{B}(r)$, we conclude that it is possible to find schemes corresponding to different classes of solution.

- One of them can be described as follows:

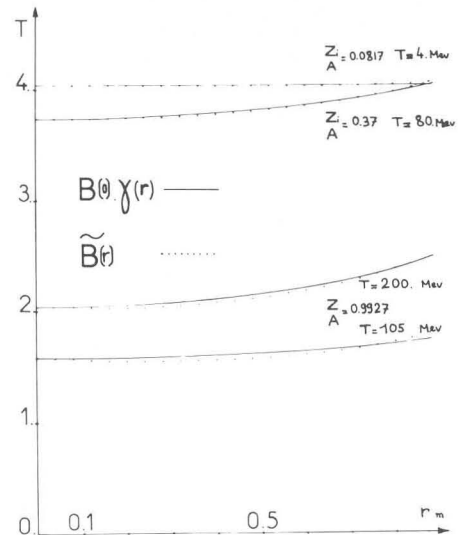


Fig. 5 : $B(o).\gamma(r)$ Laws and Isochronous average fields $\tilde{B}(r)$ as functions of the radius r . (The minimum 1.75 T flat field corresponding to $Z_1/A = 0.0816$ at 4 MeV/n has been omitted for clarity).

a) By exciting only the coil located close to the median plane, we can reach the maximum field gradient needed by the 200 MeV proton map, and adjust its absolute value by adding a constant.

b) By exciting the second and third coils in series we can obtain a field independent of the radius.

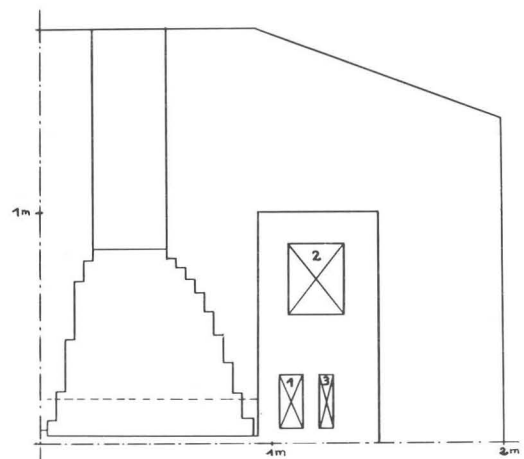


Fig. 6 : Sectional view of the magnet.

However these two coils cannot be wound at the same diameter. See Fig. (6).

Therefore, we have decided to adopt the following guidelines ;

One coil produces the gradient and other two produce the absolute value ; or more simply,

One coil creates the gradient and another is able to compensate for this gradient to produce a flat map.

Among all the possibilities for the average contribution of the iron of the pole itself to the magnetic field we chose a design to obtain a constant as a function of the radius, because there is a classical solution of that particular magnetostatic problem which is related to properties of the ellipsoid.

3.2.- Contribution of the iron of the poles

Let us consider an ellipsoid of revolution hollowed out of a soft iron cylinder of infinite height with a circular basis of radius R_p . An axial magnetisation M applied to the iron in the direction of the axis will create an uniform magnetic field BE inside the ellipsoid.

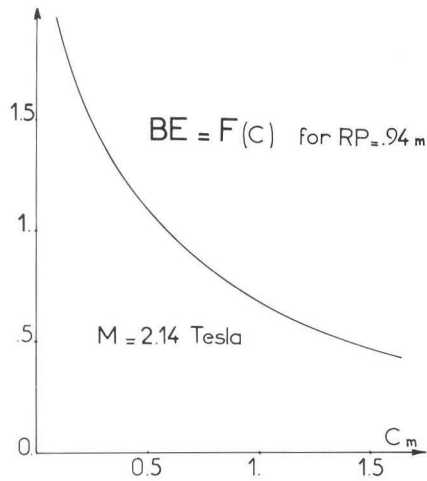


Fig.7 : Magnetostatic contribution BE of an ellipsoid of revolution with half vertical height "C" hollowed in a circular cylinder of radius R_p .

Its amplitude is related to the excentricity of the generating ellipse $BE=f(C/R_p)$, See fig.(7).

Now let us place inside 3 sectoral hills with an opening angle θ_H° , having a different elliptical profile (see fig.(8).)

We can imagine and verify by calculation that the average magnetic field in the median plane due to the magnetisation is a constant function of the radius equal to

$$\tilde{B} = \frac{BE_{HILL} \cdot \theta_H + BE_V(T - \theta_H)}{T},$$

where BE_{HILL} and BE_V are the magnetic fields of the complete ellipsoids, and T the azi-

muthal periodicity ($T = 2\pi/3$ here).

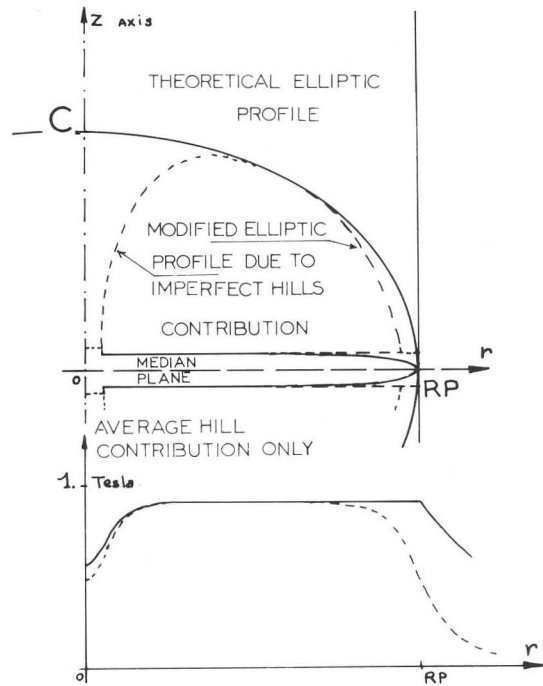


Fig.8 : Schematic section through the pole showing perfect and more realistic hill and valley profiles.

Daring to transform this expression as likely true if each term becomes a function of the radius, we obtain a means of calculating the height of the valley profile.

In our design we chose to have a mean contribution of the iron of the pole equal to $\tilde{B}(r)_{IRON POLE} = 1.3 T$. Let me point out that the lower the minimum field is, the lower must be the valley contribution. As a consequence the greater the depth of the valley and the least the desaturation effects become.

As is seen in fig (6) the shape of the valley profile is modified in the center of the machine to compensate for the lack of a hill contribution. Finally

I would like to emphasize that the property of the ellipsoid remains valid up to the pole radius if we accept a very small clearance for the extraction of the beam. This property could be used in order to investigate different extraction schemes.

3.3.- Second order assumptions

The flutter causes the average field to deviate from the $B(0) \cdot \gamma(r)$ laws within a few hundred gauss. We can calculate for each radius and particle the difference

$EC(r) = \tilde{B}(r) - B(0) \cdot \gamma(r)$ related to a given set of harmonics of the modulation. All these $EC(r)$ curves lie between two limits associated with the cross over particle $\frac{Z_i}{A} = \frac{KF}{KB}$ at maximum and minimum energy.

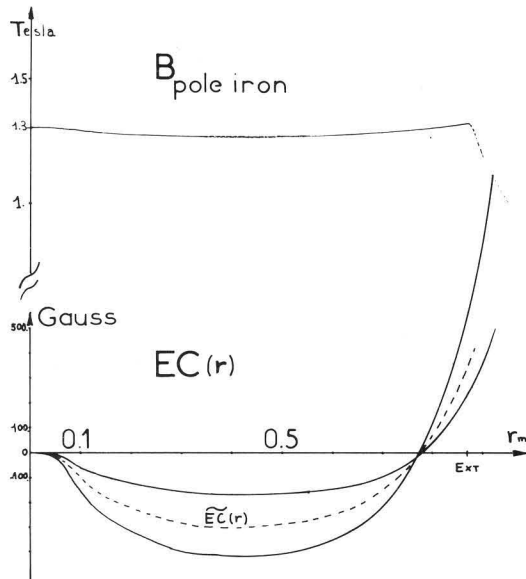


Fig.9 : Modification of a constant contribution of the pole iron taking into account the average flutter effect.

Consequently we look for a pole iron contribution not precisely equal to a constant but slightly modified and given by the following relation.

$$\tilde{B}(r)_{\text{POLE IRON}} = c^{te} + \tilde{EC}(r)$$

where $\tilde{EC}(r)$ is the mean curve shown fig.(9).

The remaining errors have to be filled by a set of correcting coils of the MSU type.

3.4.- First assumption on the yoke contribution, first check with the code "TRIM".

As a first stage we postulated that the yoke contribution was equal to the field created by the mirror image of the main coils in the horizontal parts of the yoke, one meter apart from the median plane.

In order to have a rather constant reflection coefficient $(\mu_- - 1)/(\mu_+ + 1) \approx 1$ we decide to limit the magnetic induction to 1.8 T at a radius of 1.2 m in these parts of the yoke for the maximum 4T level.

These considerations lead to a value of 0.8 meter for the thickness of this part of the yoke. See fig.(6).

Using an ellipsoid of revolution which gives the same average field of 1.3 T, we have checked with the code "TRIM" that the image procedure was not adequate and overestimates the yoke contribution (see fig.(10)).

We conclude that the yoke contribution is always low enough in our geometry

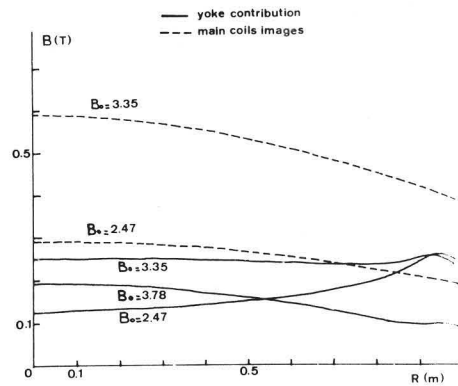


Fig.10 : Median plane yoke contribution calculated with the code TRIM at a level greater than 2.3 T. associated with a constant 1.3 T contribution of the equivalent ellipsoid.

to be disregarded for finding the position of the different parts of the main coils. Finally we will accept a slight modification of the operating diagram $J_{2,3} = f(J_1)$. See Fig.(11) to take into account the yoke contribution.

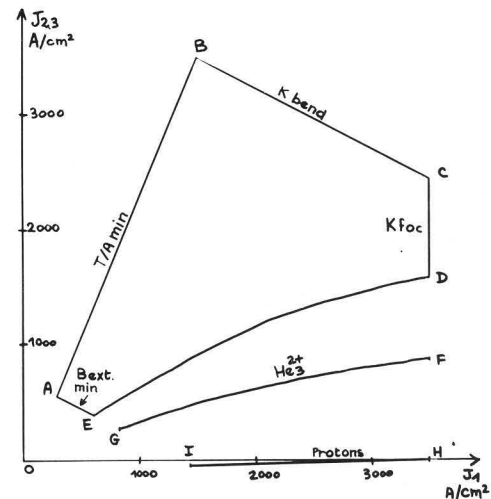


Fig.11 : Current densities functioning diagram of the main coil partition shown Fig.(6), associated with the referred points in Fig.(1)

3.5.- Refined checks using the code "TRIM"

As at other Laboratories, we have decided to make use of the code "TRIM" with a treatment of the azimuthal structure by scaling the magnetization to the fraction of the volume occupied by steel. This work is underway.

The first results are shown on Fig. 12.

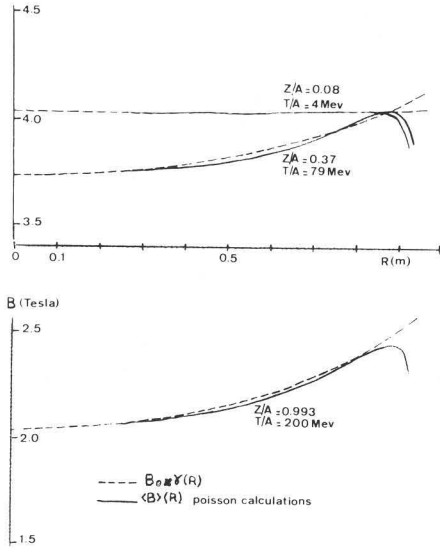


Fig. 12 : First results using stacking factors in the code "TRIM" affecting the magnetization.

4. First idea for an RF system.— The MSU, and MILANO machines have their RF design roughly in common. They consist mainly of two symmetric $\lambda/4$ resonators equipped with moving shorts. It must be clearly seen that the symmetry which avoids small vertical electric field components which could act on the beams, is paid for by a doubling of the power consumption and a cumbersome housing compared with a simple $\lambda/4$ circuit. Therefore we thought it would be relevant to make some measurements on these vertical electric field components in an unsymmetrical circuit and to make calculations on the induced motions of the beams.

Finally, I would like to mention an unexpected and interesting resonant structure which includes the power tube (avoiding the difficult low impedance coupling problems). The question was : does there exist a resonant circuit having :

- a) a constant length
- b) a constant terminal voltage ratio (+ 100.000 Volts, -16.500. Volts)
- c) two constant terminal reactances,
- d) only two parts of variable characteristic impedance in the range 5-100 Ω .

Fortunately there exists a solution to this problem which has, for the higher voltage part, a quite constant characteristic impedance. This resonator delivers a ratio of 2.5 for the maximum over minimum frequencies, in a range below 38 MHz (using the MSU K 500 RF components.)(2)

These results are summarized Fig.(13)

5. Conclusion.— These first design studies of a compact isochronous cyclotron with superconducting coils for both light and heavy ions seems to be promising enough to be considered as a useful connection between the room temperature compact isochronous cyclotrons and the first superconducting ones.

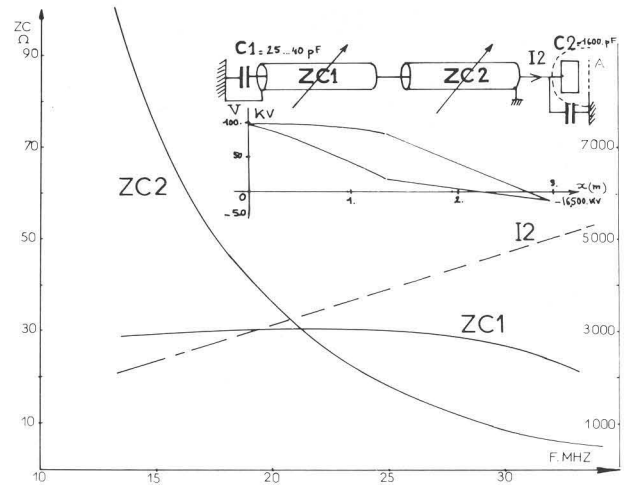


Fig. 13 : Schematic view of the resonant circuit including the power tube. Characteristic impedance ZC1 and ZC2 and terminal current I2 as function of the frequency.

Acknowledgements : The author is indebted to Professor E. ACERBI who is here gratefully acknowledged.

References :

1. J.P. SCHAPIRA, IPN Orsay. A possible design for an axial injection system into the proposed superconducting cyclotron at Orsay (contribution to this conference).
2. A. LAISNE, IPN Orsay. Pré-étude sur les structures résonnantes R.F. de cyclotrons compacts. GEPL/6/80/ACC. COMP/RF/E.

" DISCUSSION "

Y. JONGEN : How do you realize those variable impedance lines ?

A. LAISNE : I am thinking to a scheme previously used at ORSAY for the SC 200 beam stretching "C" electrode which is made of rectangular coaxial lines. The inner conductor is shaped in a very flat rectangular form, on the axis of another bigger rectangular conductor with two moving panels which provide a 5-100 Ω characteristic impedance variation.

